High-resolution near-field imaging and far-field antenna measurements with atomic sensors

David A. Anderson[*†], Eric Paradis[†§], Georg Raithel[†‡], Rachel E. Sapiro[†], Matthew T. Simons[¶],
and Christopher L. Holloway[¶]
Rydberg Technologies, Ann Arbor, MI USA[†]
University of Michigan, Ann Arbor, MI USA[‡]
Eastern Michigan University, Ypsilanti, MI USA[§]
National Institute for Standards and Technology, Boulder, CO USA[¶]
[*]dave@rydbergtechnologies.com

Abstract—**Measurements of radio-frequency (RF) electric fields using atomic sensors based on quantum-optical spectroscopy of Rydberg states in vapors has garnered significant interest in recent years for the establishment of atomic standards for RF electric fields and towards the development of novel RF sensing instrumentation. Here we describe recent work employing atomic sensors for sub-wavelength near-field imaging of a K_u-band horn antenna. We demonstrate near-field imaging capability at a spatial resolution of $\lambda/10$ and measurements over a 72 to 240 V/m field range using off-resonance AC-Stark shifts of a Rydberg-atom resonance. A fiber-coupled atomic-sensor probe is also employed in far-field measurements of a WR-90 standard gain horn.**

Index Terms—**Atomic sensors, quantum sensing, Rydberg, atom, radio-frequency, RF, microwave, electric field, metrology, antenna, antenna characterization, electromagnetic compatibility.**

I. INTRODUCTION

Atom-based sensing and measurement instrumentation for radio-frequency (RF) electric fields provides advantages over traditional antenna and solid-state detector technologies. The advantageas include small sensor sizes, absolute measurement capability (SI-based measurement), higher accuracy and precision, as well as the prospect of re-calibration-free operation, affording greater long-term measurement stability and reliability. Atomic sensors for electric fields are based on quantum-optical spectroscopy of atomic Rydberg states in vapors contained in spectroscopic cells [1]. This field measurement approach exploits the sensitivity of Rydberg atoms [2] to electric fields over a wide frequency range (MHz into the sub-THz) [3]–[7], and has garnered significant interest at National Metrology Institutes worldwide for the establishment of new atomic standards for electric fields [8]–[10], as well as in industry for the development of quantum electric-field sensing, measurement, and imaging technologies [11], [12]. Towards the establishment of new atomic electric-field standards, as well as sensors and instrumentation for metrology and RF measurement applications, the development of compact atomic sensors and probes and their implementation in high-spatial-resolution RF field measurements is desired. In this report we present recent work employing an atomic sensing element to image the near-field electric-field distribution of a K_u-band

horn antenna. We demonstrate imaging at a $\sim \lambda/10$ spatial resolution for 13.4884 GHz fields over a field range from $\sim$72 to 240 V/m. The electric-field readout is obtained by optical detection of field-induced AC-Stark shifts of atomic Rydberg resonances in the sensor. Measured field profiles are in good agreement with calculated distributions. We also demonstrate the use of a fiber-coupled atomic-sensor probe in antenna pattern measurements in the far-field of a WR-90 horn. The presented work serves to pave the way towards atomic sensors and probes for use in metrology and RF measurement applications.

II. RF ELECTRIC-FIELD MEASUREMENTS WITH ATOMIC SENSORS

In our near-field experiments, the atomic sensing element comprises a glass cell filled with a rubidium (Rb) vapor. The active sensing region of the cell has a 3-mm inner-dimension; an elongated reservoir with a sample of Rb metal is located several centimeters away. Two counter-propagating lasers at wavelengths of 780 nm and 480 nm are focused and counter-propagated through the active region of the vapor cell for electromagnetically induced transparency (EIT) spectroscopy on field-sensitive Rydberg states. The 780 nm laser is frequency stabilized to the Rb $5S_{1/2}$ to $5P_{3/2}$ transition, whose absorption through the atomic medium is measured, as the 480 nm laser frequency is scanned linearly across a range of $5P_{3/2}$ to Rydberg-state transitions. The range of states and energy ranges scanned is adapted to the field-strength and frequency ranges of the RF fields to be measured. When the 480 nm laser frequency is tuned into resonance with a transition into an RF-perturbed Rydberg state, the laser mixes the 5P and the Rydberg state. This leads to a destructive quantum interference of excitation pathways that, over a narrow frequency range at the center of the resonance, results in an increased transmission for the 780 nm light through the vapor cell. These transmission peaks serve to locate the energy levels of the RF-perturbed Rydberg levels. The RF-induced energy shifts of the Rydberg levels as well as the measured splitting patterns of the spectroscopic lines provide an excellent measure for the RF electric field strength.
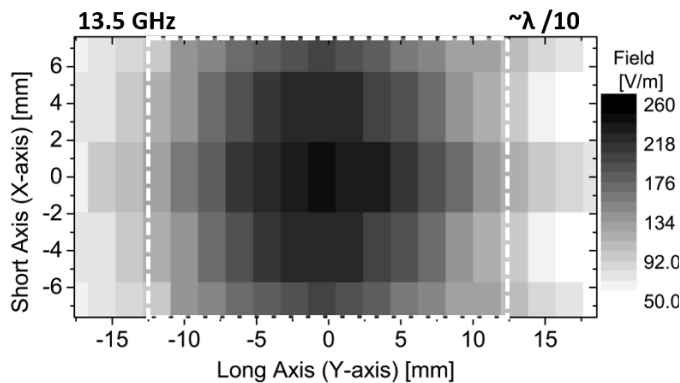
Fig. 1. Two-dimensional electric field distribution of a horn antenna, measured with an atomic sensing element on a plane of fixed distance from the horn aperture. The geometry of the horn aperture is indicated by the white dashed line.

Fig. 2. Electric field versus distance along the bore-sight of the antenna measured with the atomic sensor.

III. NEAR-FIELD IMAGING OF A HORN ANTENNA

We employ the atomic sensing element to measure the near-field of a K_u-band 0.695 x 1 inch pyramidal horn antenna emitting 13.4884 GHz fields (near-field range = 5.8 cm). The horn aperture is positioned at a distance z=7.5 mm from the sensing element and is translated in steps of 1.9 ± 0.2 mm across the long axis of the horn in the xy-plane.

Fig. 1 shows a two-dimensional spatial electric-field distribution. The image is composed of a field distribution measured over the top half of the plane and its mirror-image in the bottom half, symmetric across the short-axis zero. The electric field at each position of the horn is obtained from EIT detection of the RF-induced AC-Stark shift of the $47S_{1/2}$ Rydberg state using the relation $E = (4\Delta/\alpha)^{0.5}$, where Δ is the measured peak shift of the atomic line, and $\alpha = 4.099 \times 10^{-3}$ MHz/(V/m)^2 is the Rb 47S AC polarizability at 13.5 GHz. This relation holds in fields low enough that the field does not induce transitions, and that higher-order, non-quadratic shifts of the Rydberg level are not significant. The image shown in Fig. 1 is in good agreement with a calculated field distribution. A detailed analysis of experimental and calculated field distributions may provide insight into RF perturbations caused by the geometry and material of the vapor-cell sensing element, and is planned for upcoming work. This is a topic of particular importance in metrology applications of these atomic electric field sensors.

Fig. 2 shows measurements of the electric field as a function of distance along the bore-sight of the horn using the atomic sensor. Due to the $\sim n^7$-dependence of the atomic polarizability, the sensitivity of the atomic sensor to RF electric fields can be set by optically detecting states of different n (and other quantum numbers). The measured profile along the bore-sight of the antenna was performed with the atomic sensor using both the $47S_{1/2}$ and $40S_{1/2}$ Rydberg states. The data in Fig. 2 for the $40S_{1/2}$ case shows a near-linear decrease in field strength as a function distance away from the horn, as one would expect. The data obtained with the more sensitive
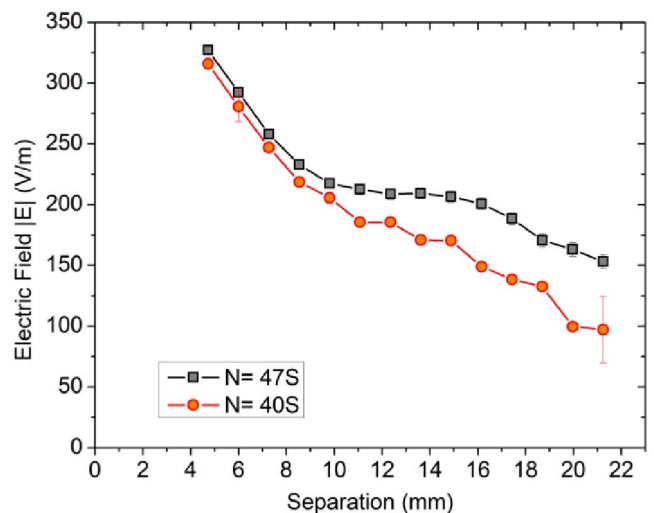
$47S_{1/2}$-state, on the other hand, exhibits a clear deviation from a linear drop-off. The measured deviation may be attributed to RF backscatter from nearby objects that could arise as the horn is translated away from the atomic sensor. In the data measured with the less sensitive $40S_{1/2}$-state this non-linear trend is seen less clearly (as one may expect from the lower sensitivity of that state). The deviations may also arise from standing-wave effects within the dielectric atomic sensing element itself, which has been seen in previous works. Simulations of this emitter and detector system are on-going to provide additional insight.

IV. FAR-FIELD ANTENNA PATTERN MEASUREMENTS

An atomic-sensor fiber-coupled probe is used to measure the antenna pattern of a Narda 640 standard gain horn antenna (mention of this product does not imply an endorsement, but serves to clarify the antenna used). The experimental setup for these measurements is shown in Fig. 3. Here, the probe was placed 0.835 m from the horn antenna in the quasi-far-field. The measurements are performed by scanning the antenna from bore-sight to an angle of 60^0. The probe measures the RF E-field across both the E-plane and H-plane of the horn antenna using Autler-Townes splittings of a Rydberg resonance [3]. Fig. 4 shows the resultant measured antenna patterns for both the E-plane and H-plane at 11.6 GHz. For comparison and validation of the atom-based measurement method, we also show results obtained at a similar frequency (9.4 GHz) in an anechoic chamber test range [13]. The comparison measurements were performed with a traditional antenna-based microwave detector. We observe very good agreement between the atom-based and traditional (antenna-based) measurements. The observed deviations are attributed to the difference in frequency and to background scatter due to the atom-based measurements having been performed in a
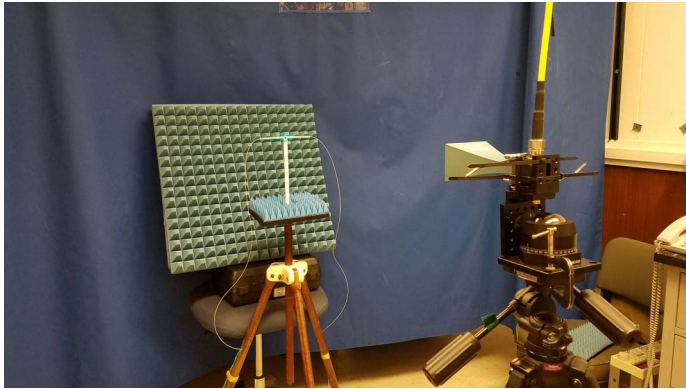
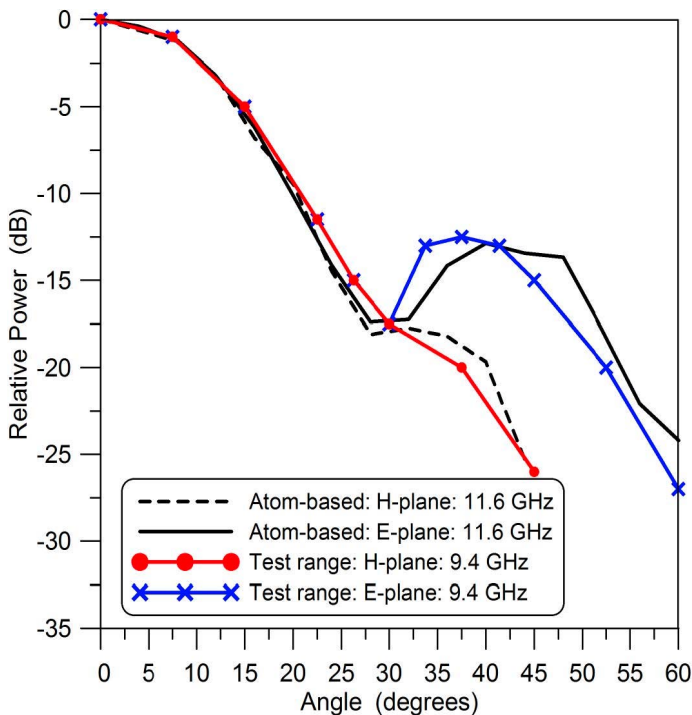Fig. 3. Setup for horn antenna pattern measurements with a fiber-coupled atom-based microwave sensor.

Fig. 4. Measured horn antenna pattern obtained with a fiber-coupled atom-based microwave sensor translated along a straight line from the horn (11.6-GHz data). For comparison and validation, we compare the atom-based data with data obtained on a traditional test range (9.4-GHZ data)

laboratory with no RF absorber on the walls and with several objects in the vicinity (see Fig. 3).

V. CONCLUSION

We report on near-field imaging of a horn antenna using a small atomic vapor cell sensing element at a resolution of $\sim \lambda/10$ and covering a dynamic field range from ~72 to 240 V/m using off-resonant AC-Stark shifts of a Rydberg resonance. The imaging results are in good agreement with calculations. We also demonstrate the implementation of a fiber-coupled atomic-sensor probe in far-field measurements of a WR-90 standard gain horn.

REFERENCES

[1] A. K. Mohapatra, T. R. Jackson, and C. S. Adams, "Coherent optical detection of highly excited rydberg states using electromagnetically induced transparency," *Phys. Rev. Lett.*, vol. 98, p. 113003, Mar 2007. [Online]. Available: http://link.aps.org/doi/10.1103/PhysRevLett.98.113003

[2] T.F.Gallagher, *Rydberg Atoms*, 1994.

[3] J. A. Sedlacek, A. Schwettmann, H. Kübler, R. Löw, T. Pfau, and J. P. Shaffer, "Microwave electrometry with rydberg atoms in a vapour cell using bright atomic resonances," *Nat. Phys.*, vol. 8, pp. 819–824, November 2012.

[4] C. Holloway, J. Gordon, S. Jefferts, A. Schwarzkopf, D. Anderson, S. Miller, N. Thaicharoen, and G. Raithel, "Broadband rydberg atom-based electric-field probe for si-traceable, self-calibrated measurements," *IEEE Transactions on Antennas and Propagation*, vol. 62, no. 12, pp. 6169–6182, Dec 2014.

[5] M. T. Simons, J. A. Gordon, C. L. Holloway, D. A. Anderson, S. A. Miller, and G. Raithel, "Using frequency detuning to improve the sensitivity of electric field measurements via electromagnetically induced transparency and autler-townes splitting in rydberg atoms," *Applied Physics Letters*, vol. 108, no. 17, p. 174101, 2016. [Online]. Available: https://doi.org/10.1063/1.4947231

[6] D. A. Anderson, S. A. Miller, G. Raithel, J. A. Gordon, M. L. Butler, and C. L. Holloway, "Optical measurements of strong microwave fields with rydberg atoms in a vapor cell," *Phys. Rev. Applied*, vol. 5, p. 034003, Mar 2016. [Online]. Available: http://link.aps.org/doi/10.1103/PhysRevApplied.5.034003

[7] S. A. Miller, D. A. Anderson, and G. Raithel, "Radio-frequency-modulated rydberg states in a vapor cell," *New Journal of Physics*, vol. 18, no. 5, p. 053017, 2016. [Online]. Available: http://stacks.iop.org/1367-2630/18/i=5/a=053017

[8] J. A. Gordon, C. L. Holloway, A. Schwarzkopf, D. A. Anderson, S. Miller, N. Thaicharoen, and G. Raithel, "Millimeter wave detection via autler-townes splitting in rubidium rydberg atomsa)," *Applied Physics Letters*, vol. 105, no. 2, pp. –, 2014. [Online]. Available: http://scitation.aip.org/content/aip/journal/apl/105/2/10.1063/1.4890094

[9] C. L. Holloway, J. A. Gordon, A. Schwarzkopf, D. A. Anderson, S. A. Miller, N. Thaicharoen, and G. Raithel, "Sub-wavelength imaging and field mapping via electromagnetically induced transparency and autler-townes splitting in rydberg atoms," *Applied Physics Letters*, vol. 104, no. 24, pp. –, 2014. [Online]. Available: http://scitation.aip.org/content/aip/journal/apl/104/24/10.1063/1.4883635

[10] C. L. Holloway, M. T. Simons, J. A. Gordon, P. F. Wilson, C. M. Cooke, D. A. Anderson, and G. Raithel, "Atom-based rf electric field metrology: From self-calibrated measurements to subwavelength and near-field imaging," *IEEE Transactions on Electromagnetic Compatibility*, vol. 59, no. 2, pp. 717–728, April 2017.

[11] D. A. Anderson and G. Raithel, "Continuous-frequency measurements of high-intensity microwave electric fields with atomic vapor cells," *Applied Physics Letters*, vol. 111, no. 5, p. 053504, 2017. [Online]. Available: http://dx.doi.org/10.1063/1.4996234

[12] (2015) Rydberg technologies. [Online]. Available: http://www.rydbergtechnologies.com

[13] T. J. Duck, B. Firanski, F. D. Lind, and D. Sipler, "Aircraft-protection radar for use with atmospheric lidars," *Appl. Opt.*, vol. 44, no. 23, pp. 4937–4945, Aug 2005. [Online]. Available: http://ao.osa.org/abstract.cfm?URI=ao-44-23-4937